Development 138, 87-96 (2011) doi:10.1242/dev.055350

Regulation of *C. elegans* presynaptic differentiation and neurite branching via a novel signaling pathway initiated by SAM-10

Qun Zheng[1], Anneliese M. Schaefer[1,2] and Michael L. Nonet[1,*]

SUMMARY

Little is known about transcriptional control of neurite branching or presynaptic differentiation, events that occur relatively late in neuronal development. Using the *Caenorhabditis elegans* mechanosensory circuit as an in vivo model, we show that SAM-10, an ortholog of mammalian single-stranded DNA-binding protein (SSDP), functions cell-autonomously in the nucleus to regulate synaptic differentiation, as well as positioning of, a single neurite branch. PLM mechanosensory neurons in *sam-10* mutants exhibit abnormal placement of the neurite branch point, and defective synaptogenesis, characterized by an overextended synaptic varicosity, underdeveloped synaptic morphology and disrupted colocalization of active zone and synaptic vesicles. SAM-10 functions coordinately with Lim domain-binding protein 1 (LDB-1), demonstrated by our observations that: (1) mutations in either gene show similar defects in PLM neurons; and (2) LDB-1 is required for SAM-10 nuclear localization. SAM-10 regulates PLM synaptic differentiation by suppressing transcription of *prk-2*, which encodes an ortholog of the mammalian Pim kinase family. PRK-2-mediated activities of SAM-10 are specifically involved in PLM synaptic differentiation, but not other *sam-10* phenotypes such as neurite branching. Thus, these data reveal a novel transcriptional signaling pathway that regulates neuronal specification of neurite branching and presynaptic differentiation.

KEY WORDS: Synapse differentiation, Neurite branching, Branch positioning, Transcriptional regulation, SAM-10, *C. elegans*

INTRODUCTION

Chemical synapses are the primary intercellular signaling unit in the nervous system. After reaching target area, axons form synapses to innervate their postsynaptic partners. The stereotypic growth pattern of axons, including branching, and precise assembly of synapses are crucial in building the complex neuronal networks of the brain. Ultrastructurally, mature synapses consist of precisely juxtaposed specialized pre- and postsynaptic subcellular structures. The presynapse consists of a cluster of synaptic vesicles that surround an electron-dense cytomatrix, the active zone, for exocytosis of transmitters. The postsynapse is highly enriched in neurotransmitter receptors and many associated scaffolding proteins, which serve to anchor the receptors in proximity to the presynaptic release site. Synapses are very stable, yet plastic. As the likely cellular site of both learning and memory, the pre- and postsynapse have the dual potential of being exceedingly stable structures, but also retain the ability to change dynamically to alter synaptic strength. Therefore, understanding the molecular mechanisms underlying assembly of synapses is crucial to understanding both brain development and function.

Studies have shown that presynaptic differentiation is regulated by intra- and extracellular signals. One type of regulatory mechanism that has been well described involves local acting post-transcriptional signals that are crucial for synaptogenesis in a variety of systems. For example, PHR (Pam/Highwire/RPM-1) proteins are evolutionarily conserved E3 ubiquitin ligases, which regulate synaptic structure and function in mice, flies and worms (Burgess et al., 2004; Nakata et al., 2005; Schaefer et al., 2000; Wan et al., 2000; Zhen et al., 2000). RPM-1, the *C. elegans* PHR, functions coordinately with the F-box protein FSN-1 to regulate synaptic differentiation by silencing the DLK-1/MKK-4/PMK-3 MAP kinase pathway at the neuromuscular junction (NMJ) (Liao et al., 2004; Nakata et al., 2005; Zhen et al., 2000). Likewise, the *Drosophila highwire* gene was also found to regulate synaptogenesis at NMJs (Wan et al., 2000). More recently, a ubiquitin-signaling pathway mediated by Cdc20-APC was shown to regulate presynaptic differentiation in mammalian neurons (Yang et al., 2009).

The use of post-translational regulation such as ubiquitin-mediated protein degradation in synaptic development provides a mechanism to overcome the difficulty of transmitting signals across extended distances between the synapse and the soma. However, regulation at the transcriptional level is also likely to play crucial roles in synaptic differentiation (Diaz, 2009; Kalinovsky and Scheiffele, 2004). In a screen for genes induced by membrane depolarization in mouse cortical neurons, Npas4 was identified as a transcription factor regulating inhibitory synapse development in an activity-dependent manner (Lin et al., 2008). In *Drosophila*, mutations in multiple components of a TGFβ/BMP signaling pathway have been identified that regulate the size of presynapses via a retrograde signaling pathway that acts via phosphorylated and nuclearly-localized SMAD (McCabe et al., 2004). Furthermore, these pathways are probably modulated at many different levels, because mutants such as *spinster* (Sweeney and Davis, 2002) and *nervous wreck* (O'Connor-Giles et al., 2008), which encode genes that regulate endocytic trafficking also display synaptogenesis defects. These studies suggest that synaptogenesis is finely tuned

[1]Department of Anatomy and Neurobiology, Washington University School of Medicine, 660 South Euclid Avenue, St Louis, MO 63110, USA. [2]Department of Neurology, Washington University School of Medicine, 660 South Euclid Avenue, St Louis, MO 63110, USA.

*Author for correspondence (nonetm@pcg.wustl.edu)

Accepted 28 October 2010

by distinct mechanisms. Although an increasing number of intrinsic signals have been implicated in regulating synaptic development, it is not yet fully understood how neurons program synaptic differentiation at the transcriptional level: namely, how neurons become competent for synaptogenesis.

One confounding factor in defining synaptogenesis is that synaptic differentiation is a late step in the differentiation of neurons. Numerous signaling pathways including many transcriptional pathways have been described; their disruption severely affects neuronal development before synaptogenesis is even initiated. For example, neuronal cell-fate specification along both the rostrocaudal and dorsoventral axes in the brain is regulated by a large number of extensively studied transcription factors and less thoroughly characterized associated factors. One such factor is Single-stranded DNA-binding protein (SSDP), which was originally isolated as a nuclear protein that specifically binds to the single-stranded polypyrimidine region of the chicken α2 (I) collagen promoter (Bayarsaihan et al., 1998). SSDP interacts biochemically with Lim domain binding protein 1 (LDB-1), which, in turn, binds to a variety of Lim homeobox transcription factors (LimHD) (Agulnick et al., 1996; Chen et al., 2002; van Meyel et al., 2003). The similarity of the embryonic lethal phenotypes of *ldb1*, *ssdp1* and some *limHD* mutants have lead to the current hypothesis that SSDP functions in a complex with LDB1 and LimHDs to regulate neuronal cell fate (Enkhmandakh et al., 2006; Nishioka et al., 2005). However, biochemical studies suggest that SSDP may also function to execute transcriptional activities independently of LDB1 (Wu, 2006).

Whereas SSDP is clearly required for late stage embryonic brain development, no studies have addressed whether SSDP is involved in neurite branching or synaptic differentiation. Here we use the *C. elegans* mechanosensory system as a model to study these processes, and describe an evolutionarily conserved signaling pathway that cell-autonomously regulates the stereotypic pattern of neurite branching and presynaptic development. This pathway consists of two nuclear components, SAM-10 (encoding a *C. elegans* ortholog of SSDP) and LDB-1. Mutations in *sam-10* or *ldb-1* disrupt neurite branching spatial pattern and synapse formation in a characteristic manner. Furthermore, we show that SAM-10/LDB-1 regulates synaptogenesis by downregulating transcription of *prk-2*, a Pim kinase gene. Overexpression of *prk-2* mimics synaptic defects observed in *sam-10* or *ldb-1* mutants; disruption of *prk-2* suppresses them. As SAM-10 translocates into the nucleus early in embryonic development well before the pre- and postsynaptic cells become juxtaposed (in the first larval stage), we propose that the *sam-10*/*ldb-1*/*prk-2* pathway may pre-program the presynaptic cell to facilitate rapid assembly of synaptic structures.

MATERIALS AND METHODS

Strains and genetics

Caenorhabditis elegans animals were maintained using standard methods (Brenner, 1974). All strains used except for those used for SNP mapping were derivatives from the Bristol N2 wild-type background. Strains used were: Bristol N2 wild type, CB4856 wild type, *jsIs821*(*mec-7$_p$:GFP-RAB-3*), *jsIs973* (*mec-7$_p$:mRFP*), *jsIs1075* (*mec-7$_p$: TagRFP-elks*); *jsIs821*, *jsIs1075; jsIs1238*(*mec-7$_p$:syd-2-GFP*), *rol-1*(*e91*) *sam-10*(*js94*) *unc-52*(*e444*) *I; jsIs821*, *sam-10*(*js94*), *sam-10*(*js94*)*; jsIs821*, *sam-10*(*js94*)*; jsIs973*, *sam-10*(*js94*)*; jsIs1075; jsIs821*, *ldb-1*(*ok896*) *jsIs821/egl-15*(*n484*) *jsIs821*, *jsIs1075; ldb-1*(*ok896*) *jsIs821*, *prk-2*(*pk278*)*; jsIs821*, *prk-2*(*pk278*)*; jsIs1075; jsIs821*, *prk-2*(*ok3069*)*; jsIs821*, *sam-10*(*js94*)*; prk-2*(*pk278*)*; jsIs821*, *sam-10*(*js94*)*; prk-2*(*pk278*)*; jsIs1075; jsIs821*, *lin-11*(*n389*)*; jsIs821*, *lim-6*(*nr2073*) *jsIs821*, *ttx-3*(*ks5*) *jsIs821*, *ceh-14*(*ch3*) *jsIs821*, *lim-7*(*tm674*) *jsIs821*, *lim-8*(*ok941*)*; jsIs821*, *lim-9*(*gk106*)*; jsIs821*, *lin-11*(*n389*)*; ceh-14*(*ch3*) *jsIs821*, *mec-3*(*e1338*)*; jsIs821*, *lyIs32* (=*whole lin-11:gfp integrant 2013*), *jsEx1079[glr-1$_p$:sam-10 cDNA rim 3′; myo-2$_p$:GFP line A]*, *jsEx1080[glr-1$_p$:sam-10 cDNA rim 3′; myo-2$_p$:GFP line D]*, *jsIs1081*(*mec-7$_p$:sam-10 cDNA rim3′; myo-2$_p$:GFP*), *jsIs1236-7[mec-7$_p$:sam-10 cDNA rim-3′ Cbunc-119]*, *jsEx1087 [sam-10$_p$:mCherry-sam-10 genomic; myo-2p:gfp, line A]; jsIs821*, *jsEx1088 [sam-10$_p$:mCherry-sam-10 genomic; myo-2$_p$:gfp, line B]; jsIs821*, *jsEx1213 [rab-3$_p$:prk-2 cDNA*)*; myo-2$_p$:gfp line A]; jsIs821. jsEx1257 [mec-7p::prk-2 cDNA* (*30ng/ul*)*; pRF4* (*rol-6*)*, line B]; jsIs821*, *juIs1*(*unc-25p:snb-1-GFP*) and *sam10*(*js94*)*; juIs1*.

Generation of transgenic animals

Transgenic animals carrying extrachromosomal arrays were generated by injecting corresponding plasmid DNA (10 ng/μl) into gonads (Mello et al., 1991) using *myo-2$_p$:gfp* (5 ng/μl) or *rol-6* (150 ng/μl) as an injection marker. *mec-7$_p$:sam-10* cDNA integrants were generated using a bombardment protocol with *Cbunc-119* as the integration marker (Praitis et al., 2001). *jsIs1081* is a spontaneous integrant line from the corresponding transgenic extrachromosomal array.

sam-10 molecular cloning

Classical three-factor genetic mapping narrowed *sam-10* mutation down to an interval between *rol-1* and *unc-52,* a region spanning 2.5 Mb on chromosome II. Single nucleotide polymorphisms (SNP) were used to position *sam-10* using CB4856 as a reference strain and narrowed the mutation down to a 58 kb region on Chromosome 2 (13,301,911 bp to 13,359,697 bp) between snp_Y48C3A[9] and snp_Y48C3A[24]. This region is covered only by the YAC clone Y48C3A. *sam-10* was identified by candidate gene sequencing in this region. A nucleotide switch (G→A) was detected in the second exon of predicted Y48C3A.8a. At the time we cloned *sam-10*, Y48C3A.9 was the predicted *C. elegans* SSDP gene in Wormbase, and this predicted gene lacked a proline-rich domain (Enkhmandakh et al., 2006) (see Fig. S5A in the supplementary material). The downstream gene Y48C3A.8 contained a proline-rich domain. We tested transgenic rescue of *sam-10* mutant phenotypes using a clone encoding only Y48C3A.9, but we observed no rescue, suggesting that this prediction is incorrect (see Fig. S5B in the supplementary material). These two predicted genes actually define a single gene. *sam-10* defects are fully rescued by a transgene expressing the currently predicted Y48C3A.8a gene, the structure of which is based upon yk292a5, a 2031bp cDNA predicted to encode a 455 amino acid protein that includes a proline-rich domain. These data identified Y48C3A.8a as *sam-10*.

Molecular biology

Plasmid DNA clones were constructed using standard molecular biology techniques. Y48C3A.9 (pNM1865) plasmid was constructed by inserting into *pBluescript SK*(+) at the *Kpn*I/*Sma*I site the Y48C3A.9 PCR product (primers: GTCTCCTCCTCTCTACCTAGGCACCACAGA and GACCTGCAGACATTGGTTGATG) digested by *Bmg*I/*Kpn*I. *sam-10* genomic clone (pNM2165) was constructed by two steps: (1) the PCR product of *sam-10* 3′ end genomic region beyond Y48C3A.9 and containing the Y48C3A.8 sequences (primers: CAAAAGTGCCGG-CTCACTAGGAAAACCCA and ATATGTCTCTAAACTCTCCGAG) was inserted into Y48C3A.9 plasmid using *Kpn*I and *Nae*I; and (2) the resulting clone was modified by replacing the small promoter region with a long promoter by PCR (primers: AAGACGCAGACACTAACGACAC and AGTCATCTCTGAAGCTAGCGATTGC) using the *Nhe*I and *Sac*II. A *rab-3$_p$:sam-10 cDNA* (pNM2120) was constructed by replacing the *eGFP* sequence in a *rab-3$_p$:eGFP rim 3′* plasmid (pRAB100) excised using *Age*I and *Sac*II with *Age*I/*Sac*II digested PCR product of a *sam-10* cDNA (primers: ATACAGCACCGGTCAATGCCGCCTCAAGTGAT-TCAG and AAGGTTTTCCGCGGTGGCTCTCACACTATGCAC), derived from *yk292a.5* plasmid (a gift from Y. Kohara). A *glr-1$_p$:sam-10 cDNA* (pNM2117) plasmid was constructed by replacing the *rab-3* promoter in *rab-3$_p$:sam-10 cDNA* with the *glr-1* promoter amplified from worm genomic DNA by PCR (primers: TGTAAACTGACCACTGCAGC and AGTGACTAGAACCGGTTGCTTTGCCTTTCTTCTCGG) and inserted using *Pst*I and *Age*I. A *mec-7$_p$:sam-10 cDNA* (pNM2112) was

constructed by replacing the *rab-3* promoter in *rab-3$_p$:sam-10 cDNA* with the *mec-7* promoter amplified from genomic DNA by PCR (primers: ACTGAATTCTGCAGATACTCAAGACAGCTCGCTG and CATTCAGTACCGGTGAACGATCTCGCGCAAGTTGC) using *Pst*I and *Age*I. A *sam-10$_p$:mCherry-sam-10* (pNM2168) plasmid was generated by inserting an *mCherry* PCR product [primers: AATAGTCAGCTAGCTATGGTGAGCAAGGGCGAGG and CATCTCTGAAGCTAGCGACTTGTACAGCTCGTCCAT; template: UAS mCherry (pNM1413, a gift from the R. Wong lab)] into the *sam-10* genomic clone (pNM2165) at the *Nhe*I site in frame. A *rab-3$_p$:prk-2 cDNA* (pNM2374) plasmid was constructed by replacing the *eGFP* region of pRAB100 with a PCR product of *prk-2* cDNA (primers: ATACAGCACCGGTATGAAGAAGCTGGCTTCACTGC and AAGGTTTTCCGCGGCTAGTCCTGCGAGAAGACGCCGC) from first strand cDNA using *Age*I and *Sac*II. A *mec-7$_p$::prk-2 cDNA* (pNM2489) plasmid was constructed by replacing the *rab-3* promoter region of pNM2374 plasmid with a PCR product of the *mec-7* promoter from the worm genomic DNA prep (primers: ACCTGCAGCCCGGGGAAATTGATACTCAAGACAGC and ATACCGGTGCTAGCGTTGCTTGAAATTTGGACCCG) using restriction sites of *Xma*I and *Nhe*I.

Light microscopy

Transgenic animals were imaged on an Olympus BX60 equipped with an EXFO 120 mercury bulb using epifluorescence using standard GFP and RFP filter set. All images were taken with a Retiga EXi CCD camera using OpenLab software and processed using Adobe Photoshop.

Quantification of synaptic varicosity extension

Size of PLM synaptic varicosities was quantified using a three-point scale based upon their length. More than 95% of wild-type varicosities have a similar size: ~5 μm long. We defined these varicosities as 'normal'. Varicosities two times longer (~10 μm) than normal varicosities were defined as 'medium extension'. Varicosities even longer (>15 μm) were defined as 'severe extension'. Scoring of animals for an individual experiment was performed by a single investigator blinded to the genotype of tested animals.

Microarray assay

Animals were grown on fresh 8P plates (Wormbook.org) until gravid. Eggs were collected by bleaching and hatched in M9 buffer overnight. L1 animals were fed on fresh food for 2 hours at room temperature, harvested and separated from worm debris using a 25 μm mesh. RNA was isolated using a standard Trizol protocol. RNA preps were stored at –80°C.

Quality of RNA preps was first estimated using Agilent 2100 Bioanalyzer. RNA was then reverse transcribed using the Genisphere Array 350 kit, which generate tagged cDNA. Resulted products were hybridized to the microarrays. Four independent high-quality RNA preparations (RIN≥7) were chosen for microarray assay using long oligomer-based spotted microarray (Washington University, St Louis, MO). For dye-swap controls, we ran a technical replicate hybridization for each pair of samples in which the dyes are reversed. Gene spots with 'found/good' signals (defined by ScanArray, channel flag 3) in all scans were chosen for gene expression analysis. The microarray dataset has been deposited in NCBI's Gene Expression Omnibus, Accession Number GSE25285.

Real-time RT-PCR assay

Total RNA preparations for the microarray assays were used for real-time RT-PCR. Reverse transcription was conducted using SuperScript III First-Strand kit (Invitrogen, Carlsbad, CA, USA). Real-time RT-PCR was run on an Applied Biosystems Prism 7000 Sequence Detection System, using SYBR GREEN kit (ABI, Foster City, CA, USA). Gene specific primers were designed with Primer Express 3.0 (ABI). Each sample was tested in triplicate. Relative changes of transcripts were analyzed by $2^{-\Delta\Delta CT}$ method (Livak and Schmittgen, 2001), using levels of *act-1* transcripts as reference.

RESULTS

The *C. elegans* mechanosensory neuronal circuit provides an in vivo model for observing the bona fide pattern of synaptic differentiation (White et al., 1986). This circuit mediates responses to mechanical stimuli, for example light touches, through gap junctions (Chalfie et al., 1985). Situated in the tail ganglia, PLMs are two of the six mechanosensory neurons, each with a long anterior-orientated neurite that runs in close apposition to the hypodermis (Chalfie and Sulston, 1981) and ends posterior to the ALM somata (Gallegos and Bargmann, 2004), the anterior analogs of PLMs (see Fig. S1 in the supplementary material). Each PLM neurite branches in the posterior portion of the body, resulting in a single 'synaptic branch' that enters the ventral nerve cord (VNC). All PLM chemical synapses with interneurons are located along the synaptic branch. These synapses appear at the light level as large synaptic varicosities. Ultrastructurally, they consist of a cluster of chemical presynapses.

The ALM neurons are located in the mid-body and extend anterior neurites toward the nose tip. Each ALM also extends a branch from the anterior neurite into the nerve ring, where it forms synaptic varicosities onto postsynaptic partners (see Fig. S1 in the supplementary material).

PLM presynaptic differentiation and neurite branch positioning are defective in *sam-10* mutants

sam-10 (Synaptic vesicle tag abnormal in mechanosensory neurons) was isolated in a compound microscope screen for mutants with defects in the morphology of PLM synaptic varicosities visualized with the synaptic marker SNB-1::GFP (A.M.S., PhD thesis, Washington University, MO, USA, 2001). We also observed presynaptic defects (increased number of synaptic puncta and synaptic vesicle accumulation) in DD motoneurons using SNB-1::GFP (*juIs1*) (see Fig. S2 in the supplementary material), indicating that *sam-10* mutations affect synaptogenesis in different classes of neurons. To further define synaptogenesis defects of *sam-10* (*js94*) mutants, we used reporters for synaptic vesicle (RAB-3) and active zone (ELKS) components. Using RAB-3::GFP (*jsIs821*) to mark synaptic vesicles (Nonet et al., 1997), we observed that PLM synapses developed inappropriately: synaptic varicosities in *sam-10* mutants are extended along the VNC, and varicosities are morphologically irregular (Fig. 1A,B,C; see Fig. S3 in the supplementary material). We never observed wild-type varicosities in *sam-10* mutants at any developmental stage.

As expected, we found that active zones in wild-type animals co-localized well with synaptic vesicles in PLM synaptic varicosities, using TagRFP::ELKS (*jsIs1075*) as an active zone marker (Fig. 1B). By contrast, we found that co-localization of active zone markers (ELKS) and synaptic vesicles was disrupted in *sam-10* mutants (Fig. 1C,D; see Fig. S3 in the supplementary material). To test if ELKS puncta represent active zones in *sam-10* mutants, we examined localization of SYD-2, another active zone marker. We found that ELKS and SYD-2 colocalized well in *sam-10* mutants (see Fig. S4 in the supplementary material), confirming that ELKS labeling identifies active zones in these animals. These data suggest that *sam-10* synapses are not properly differentiated.

We also found that the PLM synaptic branch point in wild-type animals was posterior to the vulva but, in *sam-10* mutants, the branch point was frequently anterior to the vulva (Fig. 4A). Thus, *sam-10* mutations seem to specifically affect the spatial pattern of PLM neurite branching, but not branching frequency (data not shown).

In PLM neurons, altered colocalization of synaptic components was accompanied by overextension of the synaptic branch (Fig. 1A,B,C; see Fig. S3 in the supplementary material). The branches extended two- to threefold further in the ventral cord than in the wild

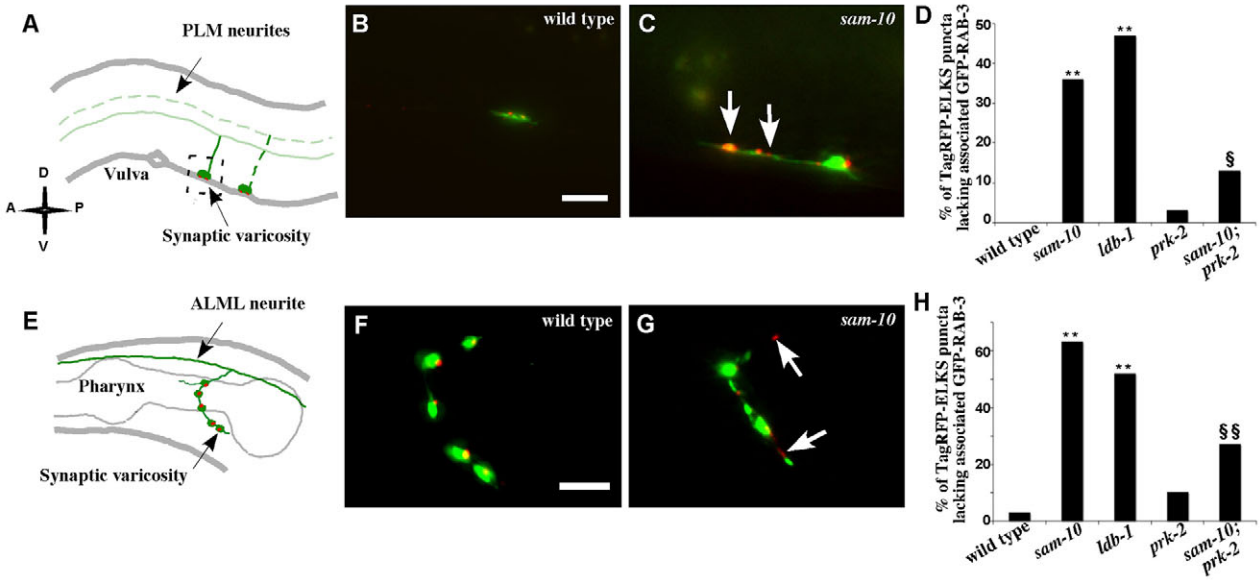

Fig. 1. Mechanosensory neuron synaptic differentiation is defective in *sam-10*(*js94*). (**A**) Diagram of PLM neurites, synaptic branches and synaptic varicosities. (**B**,**C**) Synaptic varicosities in PLM are labeled by the synaptic vesicle marker GFP-RAB-3 (green) and the active zone marker TagRFP-ELKS (red). (B) Wild-type varicosity is regularly shaped. (C) An extended, irregular shape of varicosities is often observed in *sam-10*(*js94*) mutants. ELKS puncta lacking RAB-3 are indicated (arrows). (**D**) Quantification of TagRFP-ELKS and GFP-RAB-3 marker colocalization in PLM. Fisher's exact test: $^{**}P<0.01$ (relative to wild type); $^{\S}P<0.05$ (relative to *sam-10*), $n>30$ per group. (**E**) Diagram of ALM neurites, synaptic branches and synaptic varicosities. (**F**,**G**) Synaptic varicosities in ALM are labeled by the synaptic vesicle marker GFP-RAB-3 (green) and the active zone marker TagRFP-ELKS (red). (F) Wild-type varicosities are regularly shaped. (G) An irregular shape of varicosities is often observed in *sam-10*(*js94*) mutants. ELKS puncta lacking RAB-3 are indicated (arrows). (**H**) Quantification of TagRFP-ELKS and GFP-RAB-3 marker colocalization in ALM. Fisher's exact test, $^{**}P<0.01$(relative to wild type); $^{\S\S}P<0.01$ (relative to *sam-10*), n>30 per group. Scale bar: 5 μm in B,C,F,G. A, anterior; P, posterior; D, dorsal; V, ventral.

type and they displayed more irregular 'rough' morphology. To assess whether overextension of the PLM synaptic branch is the primary cause of the colocalization defect, we examined varicosities formed in the nerve ring by the anterior mechanosensory neurons, ALM (Fig. 1E). In the nerve ring of wild-type animals, each ALM neurite formed about five synaptic varicosities along its synaptic branch; these varicosities were evenly distributed and smooth (Fig. 1F). In *sam-10* mutants, the synaptic branch extended normally into the nerve ring, and synaptic varicosities formed in the nerve ring, but individual synaptic varicosities were irregularly spaced and misshapen, although not obviously extended (Fig. 1G). Similar to PLM synaptic varicosities, colocalization of active zones and synaptic vesicles in the nerve ring was perturbed (Fig. 1G,H). These data demonstrate that mutations in *sam-10* disrupt presynaptic differentiation in *C. elegans* mechanosensory neurons, and that misalignment of synaptic components is not simply due to altered morphology of the synaptic branch.

In addition to the defects described above, *sam-10* mutants exhibited moderate uncoordinated movement (Unc), a small decrease in body size (Dpy), a defect in egg laying (Egl), and slow growth (Gro). However, they responded well to light touch (non-Mec). As the primary functional output of mechanosensory neurons is via gap junctions (Bounoutas et al., 2009; Chalfie et al., 1985), these data suggest that mechanosensory neurons are adequately differentiated and that they have formed functional gap junctions with interneurons. Consistent with the behavioral results, we found that, in *js94* mutants, PLM neurons were superficially normal in position, polarity and neurite guidance when visualized using a cytosolic monomeric RFP (mRFP) marker (*jsIs973*). These observations indicate that the defects in PLM neurons in *sam-10* mutants refer specifically to later events in neuronal development.

sam-10 encodes the *C. elegans* ortholog of mammalian SSDP

Genetic mapping narrowed the *sam-10* mutation to an interval between snp_Y48C3A[9] and snp_Y48C3A[24] on chromosome II. Sequencing of predicted gene coding regions in this interval revealed a nucleotide transition (G→A) in the second exon of predicted Y48C3A.8a. The identity of Y48C3A.8a as *sam-10* was confirmed by transgene rescue of the Sam, Gro, Unc, Dpy and Egl phenotypes. The *sam-10* phenotype was rescued by transgenic expression of a clone containing a 7 kb promoter region and the entire Y48C3A.8a coding region, but not by clones containing either a 4 kb deletion of the distal part of the promoter, or a deletion of the C-terminal portion of the Y48C3A.8a coding region (see Fig. S5 in the supplementary material; see Materials and methods for details).

Y48C3A.8a encodes a 455 amino acid protein orthologous to SSDP, which is highly conserved in *Drosophila* and mammals (Fig. 2A). Proteins of the SSDP family (Bayarsaihan, 2002) contain two conserved domains: a Forward domain that probably mediates interactions with other proteins such as LDB-1 (van Meyel et al., 2003) and a proline-rich transcriptional activating domain. The *sam-10*(*js94*) mutation introduces an early termination codon (Trp73→STOP) in the middle of the Forward domain (Fig. 2A) and probably represents a null allele of the *sam-10* gene.

SAM-10 functions cell autonomously to regulate PLM synaptic differentiation

Presynaptic differentiation can be influenced by cues derived from different sources including the presynaptic cell, postsynaptic partner(s) or neighboring support cells. To determine where SAM-10 functions to regulate presynaptic differentiation, we tested for

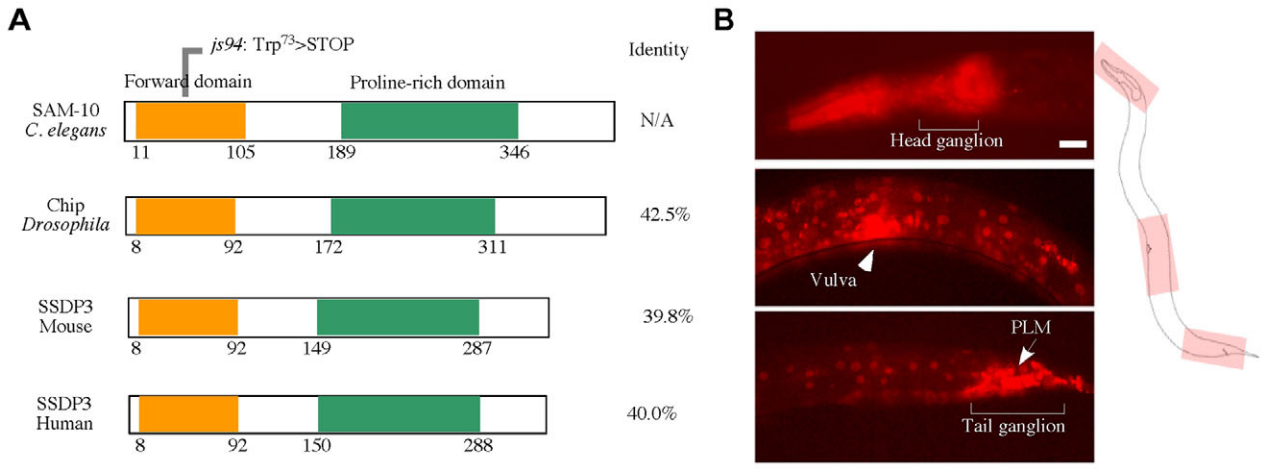

Fig. 2. *sam-10* encodes the *C. elegans* ortholog of SSDP. (**A**) SSDP is conserved in *C. elegans*, *Drosophila*, mouse and human. The Forward domain and proline-rich domains are highlighted and delineated by amino acid number. The *js94* molecular lesion is indicated. (**B**) Expression of *sam-10*$_p$*:mCherry-sam-10*. Top, expression in the head region; Middle, expression in the mid-body; Bottom, expression in the tail region. Images are focused on regions highlighted in the right diagram. Regions of the head ganglion, the vulva, the tail ganglion and the position of PLM are indicated. The signal in the pharynx is due to bleed-through of the highly expressed injection marker *myo-2*$_p$*:gfp*. Scale bar: 10 μm. N/A, not applicable.

rescue of PLM synaptic defects by expressing *sam-10* in different tissues using a transgenic approach. We found that pan-neuronal expression of *sam-10* driven by the *rab-3* promoter rescued PLM defects (three of four transgenic lines), suggesting that SAM-10 functions in neurons. We then assessed whether SAM-10 functions in the pre- or postsynaptic cells. When *sam-10* was expressed in postsynaptic partners under the *glr-1* promoter, no rescue was observed (zero of three transgenic lines). However, when we expressed *sam-10* in mechanosensory neurons using a *mec-7* promoter, PLM defects were fully rescued (three of three transgenic lines). Additionally, we noticed that *sam-10* expression in mechanosensory neurons did not rescue other *sam-10* defects including the Unc, Dpy, Egl and Gro phenotypes (data not shown), indicating that these phenotypes are independent of the function of SAM-10 in PLM late neuronal specification. These data suggest that SAM-10 functions cell-autonomously to regulate PLM presynaptic differentiation.

sam-10 is expressed broadly and localized in the nucleus of PLM

To further define the molecular mechanism underlying SAM-10 function, we characterized its expression using an *mCherry-sam-10* fusion transgene that fully rescues the *sam-10*(*js94*) phenotypes (see Fig. S5B in the supplementary material). The mCherry-SAM-10 signal was detected broadly throughout the animal with dense expression in the head ganglion, vulva and tail ganglion (Fig. 2B). This expression pattern was consistent with observed Unc, Dpy, Egl and Gro mutant phenotypes. Consistent with the cell-autonomous rescue described above, we observed *sam-10* expression in PLM neurons. Furthermore, using GFP-RAB-3 as a nuclear-excluded marker in the PLM soma, we found that SAM-10 was nuclearly localized in the PLM (Fig. 4B).

Our previous studies demonstrated that PLM synaptic branching and synaptic differentiation occur in the L1 larval stage, shortly after hatching (Schaefer et al., 2000). With this temporal framework for PLM synaptogenesis, we tested how *sam-10* expression correlated with this developmental time course. We first examined the developmental dynamics of *sam-10* expression, and found that mCherry-SAM-10 signal became detectable as early as the 1.5-fold stage during embryogenesis (Fig. 3A). However, SAM-10 is not nuclearly localized at this stage. Using RAB-3-GFP as a marker for PLMs, we discovered that SAM-10 was not nuclearly localized until the late embryonic threefold stage, just before hatching (Fig. 3B). Thus, SAM-10 translocated into the nucleus in embryonic animals, well before PLM synaptic branches have even formed in early larval stage animals, indicating that SAM-10 nuclear localization is not driven by pre- and postsynaptic cell contact.

SAM-10 and LDB-1 function coordinately to regulate PLM synaptic differentiation

In vertebrates, LDB-1 binds SSDP and plays important roles in regulating SSDP activities (Chen et al., 2002; Enkhmandakh et al., 2006; Nishioka et al., 2005). We hypothesized that SAM-10 may function in concert with the *C. elegans* ortholog of LDB-1 in regulating PLM presynaptic differentiation. *Caenorhabditis elegans ldb-1*(*ok896*) deletion mutants exhibit early larval lethality. However, a small fraction of *ok896* homozygous animals escape this lethality and grow up as sterile adults, allowing us to analyze PLM synaptogenesis in the *ldb-1* mutant background. We found that these escapers displayed similar PLM developmental defects as *sam-10*(*js94*) mutants (Fig. 1D,H; Fig. 4A), including misalignment of active zones and synaptic vesicles, anterior branch points and varicosity extension. Thus, these two proteins probably function in the same signaling pathway to regulate PLM presynaptic differentiation. Moreover, using mCherry-SAM-10 as a reporter, we found that SAM-10 failed to translocate into the PLM nucleus in *ldb-1* mutants and, instead, remained cytosolic (Fig. 4B,C). These data suggest that SAM-10 nuclear-localization, and thus its presumptive transcriptional activities, are LDB-1-dependent.

SAM-10/LDB-1 functions independently of LimHD proteins

Previous studies suggested that SSDP and LDB-1 function in a complex with LimHD to regulate different developmental pathways (Chen et al., 2002; Enkhmandakh et al., 2006; Nishioka et al., 2005). We tested whether such a complex might regulate PLM

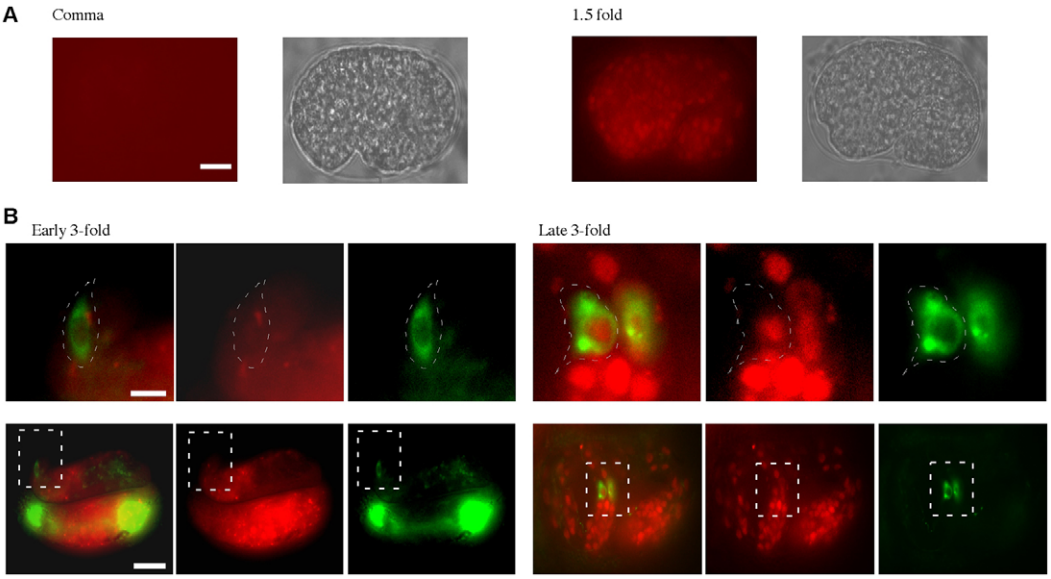

Fig. 3. Temporal expression pattern of SAM-10 during embryogenesis. (**A**) Expression of mCherry-SAM-10 becomes detectable as early as the embryonic 1.5-fold stage. Left images, mCherry-SAM-10 fluorescence; right images, corresponding bright field images of embryos. Scale: 10 μm. (**B**) mCherry-SAM-10 translocates into nucleus in the late 3-fold stage. Images on the top are a high magnification view of the area bracketed in the corresponding bottom images. RAB-3-GFP (*jsIs821*) is used as the marker of PLM neurons, outlined in the top panels. Scale bar: Top, 2.5 μm; Bottom, 10 μm.

synaptogenesis by examining the mutant phenotypes of *C. elegans* genes encoding LimHD proteins. In *C. elegans*, *mec-3* encodes a LimHD protein expressed in mechanosensory neurons (Way and Chalfie, 1988). In *mec-3*(*e1338*) mutants, PLM neurons do not differentiate properly, resulting in a Mec phenotype. Comparing the various phenotypes observed in *sam-10* and *ldb-1* animals including Gro and Unc, we found that *mec-3* mutant phenotypes were distinct (Fig. 5A). Severe PLM differentiation defects in *mec-3* mutants made it difficult to examine PLM late specifications, and also indicated that MEC-3 functions differently from SAM-10 and LDB-1, disruptions of which showed no such differentiation defects. To further confirm that MEC-3 acts distinctively from SAM-10 and LDB-1, we examined the role of these genes in regulating *mec-7* gene transcription. We found that, although *mec-7* gene transcription is disrupted in *mec-3* mutants (Duggan et al., 1998), it was not obviously affected in either *sam-10* or *ldb-1* mutants (Fig. 5A). We therefore asked if other LimHD proteins are involved in regulating late aspects of PLM differentiation by testing loss-of-function mutants of all other known *C. elegans* LimHD genes: *lin-11*, *ttx-3*, *ceh-14*, *lim-4*, *lim-6*, *lim-7*, *lim-8* and *lim-9* (Hobert and Westphal, 2000; Qadota et al., 2007). Surprisingly, none of them showed similar PLM synaptogenesis defects to *sam-10* (Fig. 5B). These observations challenge the simple model of SSDP-LDB-1-LimHD acting as a functional module, and suggest that LimHDs are probably dispensable for the SSDP-LDB-1 function in regulating PLM differentiation.

SAM-10 regulates PLM synaptic differentiation by suppressing *prk-2* expression

Previous studies and our observations of SAM-10 nuclear-localization suggest that SAM-10 might regulate PLM synaptogenesis by modifying gene expression. Therefore, we looked for downstream targets by analyzing the transcription profile changes induced by *sam-10* mutations. Because PLM synaptic differentiation occurs during the early L1 stage (Schaefer et al., 2000), we assumed that transcript levels at this developmental stage would best represent the gene expression profile involved in PLM synaptogenesis. Among regulated genes revealed by our L1 larval stage microarray analysis (see Table S1 in the supplementary material), we focused on the gene *prk-2*, the expression of which is dramatically increased in *sam-10*(*js94*) mutants. This upregulation was further confirmed by real-time RT-PCR (Fig. 6A).

Previous studies suggested that the *prk-2* gene is involved in regulating neuronal specification in *C. elegans* (Sieburth et al., 2005). We examined PLM synaptic morphology and neurite branch position in loss-of-function *prk-2* alleles *pk278* and *ok3069* (see Fig. S6A in the supplementary material). Interestingly, *prk-2* mutants seemed grossly normal in PLM synapse formation and neurite branch positioning (Fig. 1D,H; Fig. 6F,G; and data not shown). Thus, *prk-2* is not required as a positive regulator of PLM synaptogenesis.

Because *prk-2* transcription was increased in *sam-10* mutants, defects in *sam-10* mutants may result from *prk-2* overexpression. If so, loss-of-function *prk-2* mutations would be predicted to suppress these defects. We tested this hypothesis by analyzing the morphology of synaptic varicosities of ALMs and PLMs in a *sam-10*(*js94*)*; prk-2*(*pk278*) double mutant background. We found that *prk-2* loss-of-function mutations significantly suppressed synaptic defects caused by *sam-10* mutations (Fig. 1D,H; Fig. 6B). Suppression by *prk-2* mutations was incomplete, indicating that there are probably other SAM-10 regulated factors modifying synapse differentiation. Interestingly, *prk-2* mutations did not suppress other *sam-10* phenotypes (anterior branch points, Unc, Dpy or Gro) (see Fig. S6B in the supplementary material, and data not shown), suggesting that SAM-10 regulates these developmental events independently of *prk-2* transcriptional regulation.

To further confirm that increased *prk-2* expression is causal to the PLM synaptic phenotypes of *sam-10*, we tested whether overexpression of *prk-2* in wild-type animals results in *sam-10*-like phenotypes. By overexpressing *prk-2* pan-neuronally (using a *rab-3*$_p$*:prk-2* transgene) or in PLM neurons (using a *mec-7*$_p$*:prk-2*

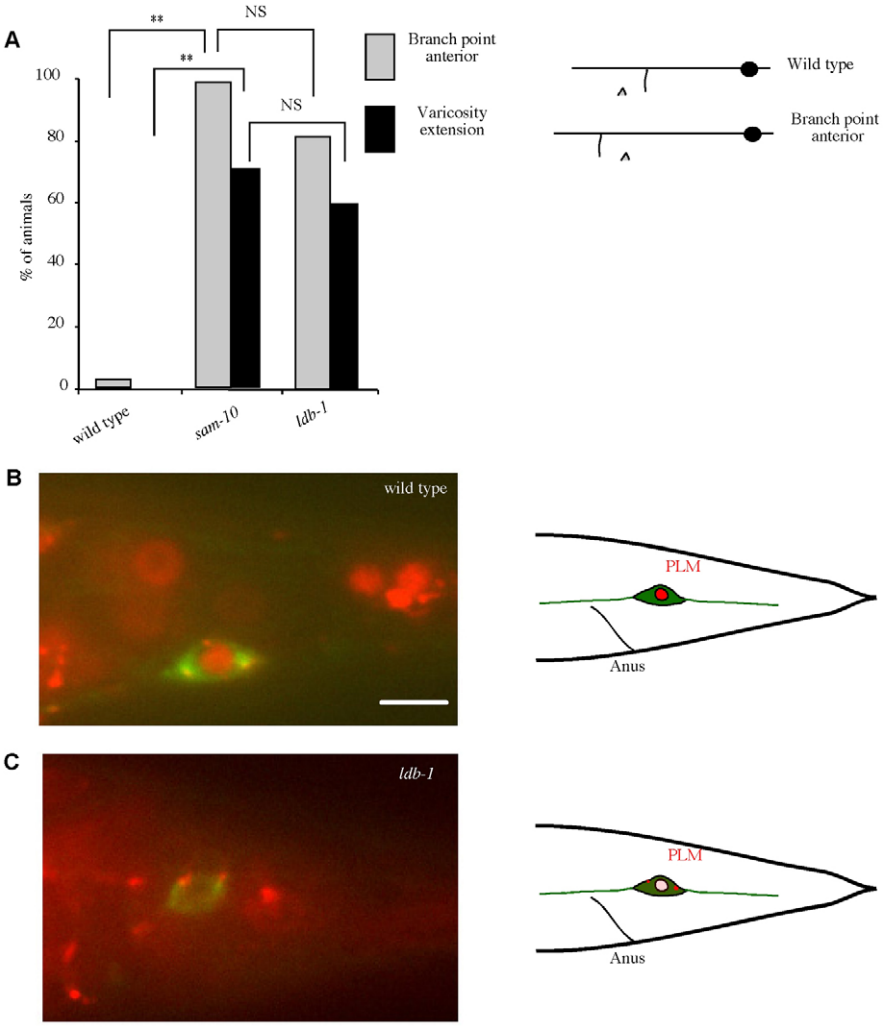

Fig. 4. SAM-10 functions coordinately with LDB-1 to regulate PLM late neuronal differentiation. (**A**) Percentage of animals with PLM synaptic branch points anterior to the vulva or extended synaptic varicosities in wild type (*n*=50), *sam-10*(*js94*) (*n*=50) and *ldb-1*(*ok896*) (*n*=10). Diagrams to the right show the PLM branch point relative to the vulva (indicated by the arrowhead). Severity of Varicosity extensions shows no detectable difference between *sam-10* and *ldb-1* mutants (data not shown). Fisher's exact test; $**P<0.01$; (**B**,**C**) Nuclear localization of mCherry-SAM-10 (red) in PLM, using GFP-RAB-3 as a nucleus exclusion marker in wild-type (B) and *ldb-1*(*ok896*) (C) animals. The PLM soma is diagrammed on the right. Scale bar: 5 μm. NS, no significance.

transgene), we found that *prk-2* overexpression caused PLM neurite overextension defects similar to those of *sam-10* mutants (Fig. 6C,D,E). Upon examining localization of synaptic vesicle and active zone markers, we found that the vesicle marker GFP-RAB-3 was broadly distributed throughout these extended varicosities, but the active zone marker remained punctate (see Fig. S6C,D in the supplementary material). Several possibilities could account for the fact that *prk-2* overexpression did not precisely recapitulate the *sam-10* PLM synaptic phenotype, including differences in the levels or temporal kinetics of PRK-2 expression, or the possibility that SAM-10 probably regulates additional signals besides PRK-2 to specify synapse differentiation. The Unc, Dpy, Gro and Egl defects seen in *sam-10* mutants were not observed in *prk-2* overexpressing animals. Taken together, these data suggest that downregulation of *prk-2* gene expression by SAM-10 is a crucial specific step in synaptic differentiation in PLM neurons.

DISCUSSION

Even though distinct pathways of transcriptional regulation have been linked with synaptogenesis (Diaz, 2009; Kalinovsky and Scheiffele, 2004), a detailed understanding of how neurons modify gene expression to instruct neurite branch positioning and synapse differentiation is lacking. Using the *C. elegans* mechanosensory system as an in vivo model, we have identified a novel signaling pathway regulating synaptogenesis that is specifically mediated by LDB-1/SAM-10/PRK-2 (Fig. 7). However, PRK-2 seems not to be required for neurite branch positioning, a process also regulated by LDB-1/SAM-10. Elucidation of these molecular cascades reveal a new facet of the complex signaling networks that regulate synaptic differentiation and neurite branching.

SSDP regulates PLM neurite branch positioning and presynaptic differentiation intrinsically at the transcriptional level

Disruption of SSDP function results in embryonic lethality in *Drosophila* and mouse models (Chen et al., 2002; Enkhmandakh et al., 2006; Nishioka et al., 2005; van Meyel et al., 2003), limiting our ability to characterize its activities during later stages of development, including neurite branch positioning and synaptic differentiation. The survival of *C. elegans sam-10* mutants allowed us to study the postembryonic functions of this protein. Our studies provide evidence that SAM-10 functions as an intrinsic signal in the nucleus to regulate neurite branch positioning and presynaptic differentiation (Fig. 7).

Regulation of the stereotypic pattern of neurite branching and growth is integral to a functional neuronal network. Owing to complexity of the mammalian nervous system, it is challenging to follow individual neurite branches, especially their spatial patterns, in vivo. Many studies on neurite branching have focused on the branching frequency. It is largely unknown how stereotypic

A

	mec-3(e1338)	*sam-10(js94)*	*ldb-1(ok896)*
PLM morphology*	Defective	Normal	Normal
Mec	Yes	No	ND
Gro	No	Yes	Yes
Unc	No	Yes	Yes
Egl	No	Yes	ND
mec-7 transcription**	Defective	Normal	Normal

*morphology at hatch
**tested with *jsIs821*

B

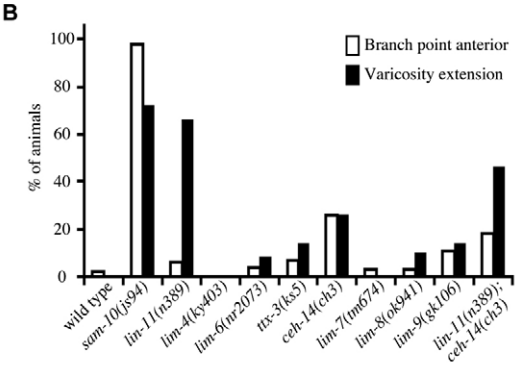

Fig. 5. *Caenorhabditis elegans* LimHD genes tested are not involved in PLM specifications regulated by *sam-10/ldb-1*.
(**A**) Distinctive phenotypes of *mec-3, sam-10* and *ldb-1 mutants*. (**B**) Effects of Lim-HD gene mutations on PLM synaptic branch positioning and synaptic varicosity extension. All varicosity extensions of *lim* mutants fall in the 'medium extension' class (see Materials and methods). *lin-11*(*n389*) causes a dramatic increase of varicosity extension. However, a close look revealed that this diffusion appears different from extended varicosities in *sam-10*(*js94*): they are more regular and even in shape and shorter than *sam-10*(*js94*) varicosities. Plus, we failed to detect LIN-11 expression in PLM neurons, *using lyIs32* (*whole lin-11::gfp integrant 2013,* a gift from Piali Sengupta). We believe that varicosity extension is probably due to VNC defects in *lin-11*(*n389*) (Hutter, 2003). Varicosity extensions in other mutants are similar to these in *lin-11*(*n389*), albeit at lower frequency as shown in the figure. *mec-3* mutants are not scored for PLM synaptic varicosity morphology owing to defective PLM neuronal differentiation. ND, not determined.

patterns of neurite branching are regulated. The consistent stereotypic pattern of *C. elegans* PLM neurite branching provides an in vivo model to study this process. We observed that SAM-10 is required in the nucleus for normal PLM neurite branch positioning but not branching frequency (*sam-10* PLM neurites, like wild-type PLM neurites, form a single branch; data not shown). However, PRK-2, a downstream signal of LDB-1/SAM-10, seems not to be involved in this regulation.

Transcriptional control of synaptic differentiation has been implicated in *Drosophila* NMJ development. Currently, two transcriptional mechanisms have been shown to be involved in this process: namely, the WNT and TGF-beta/BMP signaling pathways (Kalinovsky and Scheiffele, 2004). Triggered by pre- and postsynaptic interactions, ligands for both pathways bind to their receptors on the pre- and/or postsynaptic membrane to regulate gene expression associated with synaptogenesis (Kalinovsky and Scheiffele, 2004; Salinas, 2003). However, the molecular pathway we describe here occurs before pre- and postsynaptic contact, indicating that active transcription, translation and transport of synaptic components precedes pre-postsynaptic contacting. Further, we previously found that presynaptic specialization, characterized by active zone formation and synaptic vesicle accumulation, occurs within 30 to 60 minutes after pre- and postsynaptic contact (M. L. Nonet, unpublished observations), a time window allowing assembly of pre-existing synaptic components but not the synthesis and transport of new synaptic components. These observations suggest that at least some aspects of synapse development might be pre-programmed. Unlike the WNT and TGF-beta/BMP pathways, initiation of SAM-10 signaling appears to be independent of postsynaptic signals. We propose that SAM-10 signaling may function to pre-program PLM neuronal development for synaptogenesis.

SAM-10 regulates PLM neurite branching and presynaptic differentiation coordinately with LDB-1, but independently of *C. elegans* LimHD orthologs

SSDP-LDB-1-LimHD is hypothesized to function as a module to regulate many development processes, including neuronal development (Agulnick et al., 1996; Enkhmandakh et al., 2006; Mukhopadhyay et al., 2003; Nishioka et al., 2005; van Meyel et al., 2003). This complex is proposed based on the observations that: (1) LDB1 binds LimHD proteins; (2) LDB1 binds SSDP proteins; and (3) disruption of these components result in comparable embryonic lethality. However, no biochemical evidence directly shows the integrity of this complex. LDB1 has been shown to regulate neuronal development in *Drosophila* and mouse models. In mice, the *ldb1* gene is expressed in the developing nervous system (Agulnick et al., 1996; Bulchand et al., 2003; Ostendorff et al., 2006). Detailed analysis revealed that reductions in *ssdp1* expression or *ldb1* ablation cause remarkably similar brain developmental defects, shown by various brain regional molecular markers such as Six2 (forebrain marker), En2 (mid-hindbrain boundary marker) and Krox20 (hindbrain marker) (Mukhopadhyay et al., 2003; Nishioka et al., 2005). Similar to its mammalian orthologs, *Drosophila* Chip (ortholog of LDB1) is expressed in the developing nervous system (Morcillo et al., 1997; van Meyel et al., 2000). Loss-of-function *Chip* mutations result in defective neurotransmitter production and axon guidance (van Meyel et al., 2000). Whereas LDB-1 activities are proposed to be associated with LimHD proteins, there is also some evidence to show that LDB1 may sometimes function independently of LimHD proteins. For example, during mouse late embryonic brain development, LDB1 shows a different expression pattern from the LimHD proteins (Bulchand et al., 2003). Similarly, *Drosophila* Chip appears to have broader activities than those mediated by interactions with LimHD proteins (Morcillo et al., 1997). These studies suggest that LDB1 functions with SSDP to regulate neuronal development, and that at least some aspects of this regulation are LimHD independent.

In this study, although we show that SSDP functions coordinately with LDB-1 to regulate PLM development, our phenotypic analyses suggest that this regulation is independent of known *C. elegans* LimHD proteins (Fig. 7). However, because *mec-3* loss-of-function disrupts mechanosensory cell fate specification, a prelude to synapse formation, we cannot exclude the possibility that MEC-3 may play a role in PLM neurite branch positioning and presynaptic differentiation regulated by SAM-10/LDB-1.

SAM-10 regulates PLM synaptic differentiation by suppressing *prk-2* expression

In searching for SAM-10 downstream targets, we have shown that SAM-10 regulates PLM synaptic differentiation by inhibiting *prk-2* transcription. *prk-2* encodes a *C. elegans*

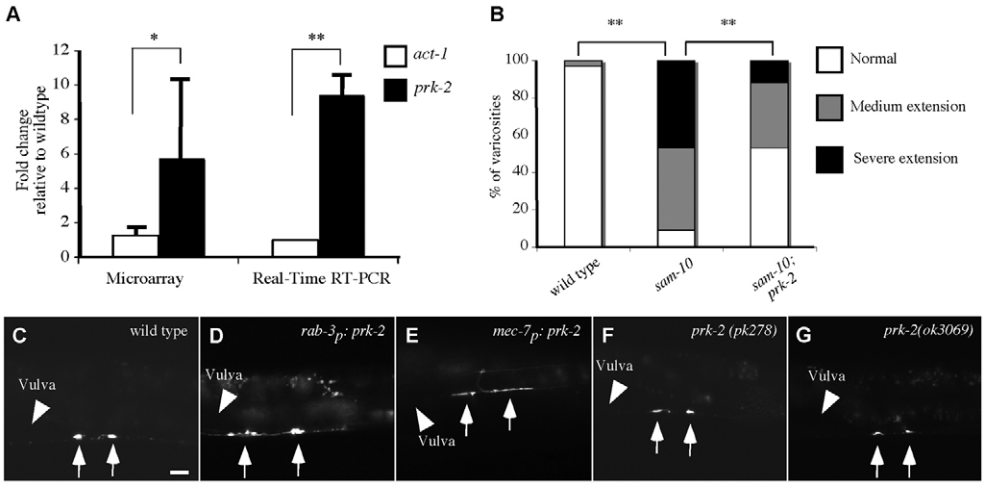

Fig. 6. SAM-10 regulates PLM synaptic differentiation by suppressing *prk-2* expression. (**A**) Increased *prk-2* transcription in *sam-10*(*js94*) revealed by microarray and real-time RT-PCR assays. *act-1* is used as a control. Student's *t*-test, **P*<0.05, ***P*<0.01, four biological repeats for microarray assay, and three repeats for real time RT-PCR assay. Error bars represent s.d. (**B**) Loss-of-function *prk-2* mutations suppress PLM synaptic defects of *sam-10*(*js94*) mutants. PLM synaptic varicosities in different genetic backgrounds are scored blindly by their length: length of wild-type varicosities (~5 μm) is defined as normal; twofold longer (~10 μm) as medium extension; and threefold longer or more (>15 μm) as severe extension (see also Materials and methods). Fisher's exact test; ***P*<0.01; *n*>30 per group. (**C-G**) PLM synaptic varicosity pattern, represented by GFP-RAB-3, in wild-type (C), *rab-3*$_p$*:prk-2* transgenic (D), *mec-7*$_p$*:prk-2* transgenic (E), *prk-2*(*pk278*) (F) and *prk-2*(*ok3069*) (G) animals. Arrows, PLM synaptic varicosities. Scale bar: 10 μm.

ortholog of the Pim kinase family, which includes three genes in mammals: *Pim1*, *Pim2* and *Pim3*. These Pim kinase genes were initially identified as oncogenic serine/threonine kinases associated with lymophoid tumors (White, 2003). In vitro studies (Feldman et al., 1998; Konietzko et al., 1999; Liu et al., 2003) demonstrated that *Pim1* and *Pim3* are among the immediate early genes induced by neuron depolarization, but not by neurotrophins or growth factors such as NGF and EGF, indicating that they may be involved in synaptic plasticity. In vivo studies (Feldman et al., 1998; Konietzko et al., 1999) showed that *Pim1* and *Pim3* expression is induced by LTP-producing stimuli in the brain. Consistent with our observations that *prk-2* mutants show no obvious defects in PLM neurons, *Pim1* knockout mice are superficially normal in development and brain morphology at the light and electron microscopic levels (Laird et al., 1993). However, these knockout mice are incapable of establishing enduring LTP, even though they show normal forms of short-term plasticity (Konietzko et al., 1999).

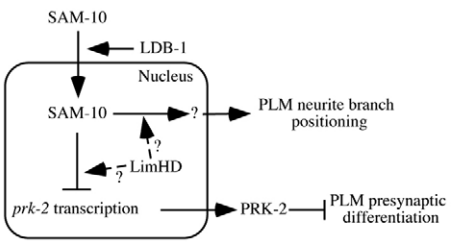

Fig. 7. Model of SAM-10 signaling pathway. SAM-10 is translocated into the nucleus in an LDB-1-dependent manner. In the nucleus, SAM-10 regulates PLM synaptic differentiation and neurite branch positioning, presumably by regulating gene expression. SAM-10 regulation of synaptic differentiation is mediated at least partially by suppressing *prk-2* transcription.

Induction of LTP is accompanied by synaptic structural plasticity, which is characterized by a dramatic increase in the proportion of axon terminals contacting multiple dendritic spines (Toni et al., 1999). It is likely that *pim* kinase genes, as immediate early genes induced by LTP-production stimuli, are involved in inducing synaptic structural plasticity by regulating presynaptic varicosity remodeling. In *C. elegans*, PLM synaptic varicosity extension induced by *prk-2* overexpression may be the result of cellular changes favoring formation of synaptic contacts with additional postsynaptic partners. Although *C. elegans* PRK-2 functions in de novo synaptogenesis and vertebrate Pim kinase functions in synaptic remodeling, these two processes probably share many features in common. Crucial to elucidating this molecular pathway will be identification of PRK-2 targets. Our system provides several genetic avenues to address this challenge.

Taken together, our observations suggest that the LDB-1/SAM-10/PRK-2 pathway represents a novel transcriptional mechanism that regulates synaptic differentiation in the *C. elegans* mechanosensory system (Fig. 7). However, it is not the first kinase pathway identified that regulates synaptogenesis. An RPM-1/MAP kinase also plays crucial roles in mechanosensory synapse development. That both signaling systems rely on kinases provides a simple mechanism for cross regulation of the two pathways. Whereas the severity and pleiotropy of the *sam-10* mutants complicates direct assessment of interactions between these pathways, cell specific transgenic approaches should eventually permit this analysis. Further investigation of this novel pathway should provide a new perspective on regulation of presynaptic differentiation.

Acknowledgements
We are grateful to CGC and P. Sengupta for providing strains used in this study; to Y. Kohara for providing the yk292a5 cDNA clone; and to G. Garriga and C. M. Crowder for critical reading of the manuscript. This work was supported award number NS040094 from NINDS. The content is solely the

responsibility of the authors and does not necessarily represent the official views of the NINDS or the National Institutes of Health. Deposited in PMC for release after 12 months.

Competing interests statement

The authors declare no competing financial interests.

Supplementary material

Supplementary material for this article is available at http://dev.biologists.org/lookup/suppl/doi:10.1242/dev.055350/-/DC1

References

Agulnick, A. D., Taira, M., Breen, J. J., Tanaka, T., Dawid, I. B. and Westphal, H. (1996). Interactions of the LIM-domain-binding factor Ldb1 with LIM homeodomain proteins. *Nature* **384**, 270-227.

Bayarsaihan, D. (2002). SSDP1 gene encodes a protein with a conserved N-terminal FORWARD domain. *Biochim. Biophys. Acta* **1599**, 152-155.

Bayarsaihan, D., Soto, R. J. and Lukens, L. N. (1998). Cloning and characterization of a novel sequence-specific single-stranded-DNA-binding protein. *Biochem. J.* **331**, 447-452.

Bounoutas, A., Zheng, Q., Nonet, M. L. and Chalfie, M. (2009). mec-15 encodes an F-box protein required for touch receptor neuron mechanosensation, synapse formation and development. *Genetics* **183**, 607-617, 1SI-4SI.

Brenner, S. (1974). The genetics of Caenorhabditis elegans. *Genetics* **77**, 71-94.

Bulchand, S., Subramanian, L. and Tole, S. (2003). Dynamic spatiotemporal expression of LIM genes and cofactors in the embryonic and postnatal cerebral cortex. *Dev. Dyn.* **226**, 460-469.

Burgess, R. W., Peterson, K. A., Johnson, M. J., Roix, J. J., Welsh, I. C. and O'Brien, T. P. (2004). Evidence for a conserved function in synapse formation reveals Phr1 as a candidate gene for respiratory failure in newborn mice. *Mol. Cell. Biol.* **24**, 1096-1105.

Chalfie, M. and Sulston, J. (1981). Developmental genetics of the mechanosensory neurons of Caenorhabditis elegans. *Dev. Biol.* **82**, 358-370.

Chalfie, M., Sulston, J. E., White, J. G., Southgate, E., Thomson, J. N. and Brenner, S. (1985). The neural circuit for touch sensitivity in Caenorhabditis elegans. *J. Neurosci.* **5**, 956-964.

Chen, L., Segal, D., Hukriede, N. A., Podtelejnikov, A. V., Bayarsaihan, D., Kennison, J. A., Ogryzko, V. V., Dawid, I. B. and Westphal, H. (2002). Ssdp proteins interact with the LIM-domain-binding protein Ldb1 to regulate development. *Proc. Natl. Acad. Sci. USA* **99**, 14320-14325.

Diaz, E. (2009). From microarrays to mechanisms of brain development and function. *Biochem. Biophys. Res. Commun.* **385**, 129-131.

Duggan, A., Ma, C. and Chalfie, M. (1998). Regulation of touch receptor differentiation by the Caenorhabditis elegans mec-3 and unc-86 genes. *Development* **125**, 4107-4119.

Enkhmandakh, B., Makeyev, A. V. and Bayarsaihan, D. (2006). The role of the proline-rich domain of Ssdp1 in the modular architecture of the vertebrate head organizer. *Proc. Natl. Acad. Sci. USA* **103**, 11631-11636.

Feldman, J. D., Vician, L., Crispino, M., Tocco, G., Marcheselli, V. L., Bazan, N. G., Baudry, M. and Herschman, H. R. (1998). KID-1, a protein kinase induced by depolarization in brain. *J. Biol. Chem.* **273**, 16535-16543.

Gallegos, M. E. and Bargmann, C. I. (2004). Mechanosensory neurite termination and tiling depend on SAX-2 and the SAX-1 kinase. *Neuron* **44**, 239-249.

Hobert, O. and Westphal, H. (2000). Functions of LIM-homeobox genes. *Trends Genet.* **16**, 75-83.

Hutter, H. (2003). Extracellular cues and pioneers act together to guide axons in the ventral cord of C. elegans. *Development* **130**, 5307-5318.

Kalinovsky, A. and Scheiffele, P. (2004). Transcriptional control of synaptic differentiation by retrograde signals. *Curr. Opin. Neurobiol.* **14**, 272-279.

Konietzko, U., Kauselmann, G., Scafidi, J., Staubli, U., Mikkers, H., Berns, A., Schweizer, M., Waltereit, R. and Kuhl, D. (1999). Pim kinase expression is induced by LTP stimulation and required for the consolidation of enduring LTP. *EMBO J.* **18**, 3359-3369.

Laird, P. W., van der Lugt, N. M., Clarke, A., Domen, J., Linders, K., McWhir, J., Berns, A. and Hooper, M. (1993). In vivo analysis of Pim-1 deficiency. *Nucleic Acids Res.* **21**, 4750-4755.

Liao, E. H., Hung, W., Abrams, B. and Zhen, M. (2004). An SCF-like ubiquitin ligase complex that controls presynaptic differentiation. *Nature* **430**, 345-350.

Lin, Y., Bloodgood, B. L., Hauser, J. L., Lapan, A. D., Koon, A. C., Kim, T. K., Hu, L. S., Malik, A. N. and Greenberg, M. E. (2008). Activity-dependent regulation of inhibitory synapse development by Npas4. *Nature* **455**, 1198-1204.

Liu, W., Feldman, J. D., Machado, H. B., Vician, L. J. and Herschman, H. R. (2003). Expression of depolarization-induced immediate early gene proteins in PC12 cells. *J. Neurosci. Res.* **72**, 670-678.

Livak, K. J. and Schmittgen, T. D. (2001). Analysis of relative gene expression data using real-time quantitative PCR and the 2(-Delta Delta C(T)) Method. *Methods* **25**, 402-408.

McCabe, B. D., Hom, S., Aberle, H., Fetter, R. D., Marques, G., Haerry, T. E., Wan, H., O'Connor, M. B., Goodman, C. S. and Haghighi, A. P. (2004). Highwire regulates presynaptic BMP signaling essential for synaptic growth. *Neuron* **41**, 891-905.

Mello, C. C., Kramer, J. M., Stinchcomb, D. and Ambros, V. (1991). Efficient gene transfer in C.elegans: extrachromosomal maintenance and integration of transforming sequences. *EMBO J.* **10**, 3959-3970.

Morcillo, P., Rosen, C., Baylies, M. K. and Dorsett, D. (1997). Chip, a widely expressed chromosomal protein required for segmentation and activity of a remote wing margin enhancer in Drosophila. *Genes Dev.* **11**, 2729-2740.

Mukhopadhyay, M., Teufel, A., Yamashita, T., Agulnick, A. D., Chen, L., Downs, K. M., Schindler, A., Grinberg, A., Huang, S. P., Dorward, D. et al. (2003). Functional ablation of the mouse Ldb1 gene results in severe patterning defects during gastrulation. *Development* **130**, 495-505.

Nakata, K., Abrams, B., Grill, B., Goncharov, A., Huang, X., Chisholm, A. D. and Jin, Y. (2005). Regulation of a DLK-1 and p38 MAP kinase pathway by the ubiquitin ligase RPM-1 is required for presynaptic development. *Cell* **120**, 407-420.

Nishioka, N., Nagano, S., Nakayama, R., Kiyonari, H., Ijiri, T., Taniguchi, K., Shawlot, W., Hayashizaki, Y., Westphal, H., Behringer, R. R. et al. (2005). Ssdp1 regulates head morphogenesis of mouse embryos by activating the Lim1-Ldb1 complex. *Development* **132**, 2535-2546.

Nonet, M. L., Staunton, J. E., Kilgard, M. P., Fergestad, T., Hartwieg, E., Horvitz, H. R., Jorgensen, E. M. and Meyer, B. J. (1997). Caenorhabditis elegans rab-3 mutant synapses exhibit impaired function and are partially depleted of vesicles. *J. Neurosci.* **17**, 8061-8073.

O'Connor-Giles, K. M., Ho, L. L. and Ganetzky, B. (2008). Nervous wreck interacts with thickveins and the endocytic machinery to attenuate retrograde BMP signaling during synaptic growth. *Neuron* **58**, 507-518.

Ostendorff, H. P., Tursun, B., Cornils, K., Schluter, A., Drung, A., Gungor, C. and Bach, I. (2006). Dynamic expression of LIM cofactors in the developing mouse neural tube. *Dev. Dyn.* **235**, 786-791.

Praitis, V., Casey, E., Collar, D. and Austin, J. (2001). Creation of low-copy integrated transgenic lines in Caenorhabditis elegans. *Genetics* **157**, 1217-1226.

Qadota, H., Mercer, K. B., Miller, R. K., Kaibuchi, K. and Benian, G. M. (2007). Two LIM domain proteins and UNC-96 link UNC-97/pinch to myosin thick filaments in Caenorhabditis elegans muscle. *Mol. Biol. Cell* **18**, 4317-4326.

Salinas, P. C. (2003). Synaptogenesis: Wnt and TGF-beta take centre stage. *Curr. Biol.* **13**, R60-R62.

Schaefer, A. M., Hadwiger, G. D. and Nonet, M. L. (2000). rpm-1, a conserved neuronal gene that regulates targeting and synaptogenesis in C. elegans. *Neuron* **26**, 345-356.

Sieburth, D., Ch'ng, Q., Dybbs, M., Tavazoie, M., Kennedy, S., Wang, D., Dupuy, D., Rual, J. F., Hill, D. E., Vidal, M. et al. (2005). Systematic analysis of genes required for synapse structure and function. *Nature* **436**, 510-517.

Sweeney, S. T. and Davis, G. W. (2002). Unrestricted synaptic growth in spinster-a late endosomal protein implicated in TGF-beta-mediated synaptic growth regulation. *Neuron* **36**, 403-416.

Toni, N., Buchs, P. A., Nikonenko, I., Bron, C. R. and Muller, D. (1999). LTP promotes formation of multiple spine synapses between a single axon terminal and a dendrite. *Nature* **402**, 421-425.

van Meyel, D. J., O'Keefe, D. D., Thor, S., Jurata, L. W., Gill, G. N. and Thomas, J. B. (2000). Chip is an essential cofactor for apterous in the regulation of axon guidance in Drosophila. *Development* **127**, 1823-1831.

van Meyel, D. J., Thomas, J. B. and Agulnick, A. D. (2003). Ssdp proteins bind to LIM-interacting co-factors and regulate the activity of LIM-homeodomain protein complexes in vivo. *Development* **130**, 1915-1925.

Wan, H. I., DiAntonio, A., Fetter, R. D., Bergstrom, K., Strauss, R. and Goodman, C. S. (2000). Highwire regulates synaptic growth in Drosophila. *Neuron* **26**, 313-329.

Way, J. C. and Chalfie, M. (1988). mec-3, a homeobox-containing gene that specifies differentiation of the touch receptor neurons in C. elegans. *Cell* **54**, 5-16.

White, E. (2003). The pims and outs of survival signaling: role for the Pim-2 protein kinase in the suppression of apoptosis by cytokines. *Genes Dev.* **17**, 1813-1816.

White, J. G., Southgate, E., Thomson, J. N. and Brenner, S. (1986). The structure of the nervous system of the nematode Caenorhabditis elegans. *Philos. Trans. R. Soc. Lond. B Biol. Sci.* **314**, 1-340.

Wu, L. (2006). Structure and functional characterization of single-strand DNA binding protein SSDP1: carboxyl-terminal of SSDP1 has transcription activity. *Biochem. Biophys. Res. Commun.* **339**, 977-984.

Yang, Y., Kim, A. H., Yamada, T., Wu, B., Bilimoria, P. M., Ikeuchi, Y., de la Iglesia, N., Shen, J. and Bonni, A. (2009). A Cdc20-APC ubiquitin signaling pathway regulates presynaptic differentiation. *Science* **326**, 575-578.

Zhen, M., Huang, X., Bamber, B. and Jin, Y. (2000). Regulation of presynaptic terminal organization by C. elegans RPM-1, a putative guanine nucleotide exchanger with a RING-H2 finger domain. *Neuron* **26**, 331-343.